IAC-22, B6,5,3, x73724

Environmental impact of large constellations through a debris index analysis

Andrea Muciaccia[a]*, Mirko Trisolini[a], Lorenzo Giudici[a], Camilla Colombo[a], Borja Del Campo[b], Francesca Letizia[c]

[a] *Department of Aerospace Science and Technology, Politecnico di Milano, Via Giuseppe La Masa 34, 20156, Milan, Italy,* andrea.muciaccia@polimi.it
[b] *Deimos Space UK Ltd., AIRSPEED 1, 151 Eighth Street, Harwell Campus, Oxfordshire, United Kingdom*
[c] *European Space Agency, Space Debris Office, Robert-Bosch-Str. 5, 64293 Darmstadt, Germany*

* Corresponding Author

Abstract

In recent years, the number of objects orbiting around the Earth has experienced a continuous growth because of the increase in the number of launches and of space debris produced by fragmentation events. This growth will likely accelerate with the introduction of large constellations in Low Earth Orbit (LEO), unless mitigating measures will be taken. Despite the benefits they will introduce, large constellations will also have a massive influence on the short- and long-term stability of the space environment, by increasing the interaction with the background space debris population and, thus, the probability of hazardous collision events. New mitigation policies and a careful mission design including the post mission disposal are required for ensuring a future sustainable access to space.

This work aims at analysing how the inclusion of large constellations will affect the population of objects already in-orbit. Indeed, the inclusion of a large number of objects in restricted region of the space will change the future population shape. Then, the impact of a constellation is evaluated taking as reference the OneWeb constellation, already being deployed. The evaluation is performed using the THEMIS software tool, developed at Politecnico di Milano in collaboration with Deimos Space within an ESA-funded project. In this frame, the impact of a mission on the space environment is assessed considering the likelihood and associated effects of fragmentations of the satellite(s) during each phase of the mission.

Keywords: Constellations**,** Environmental impact, Debris index, Low Earth Orbit

Acronyms/Abbreviations

CAM	Collision Avoidance Manoeuvre
EOL	End of Life
ESA	European Space Agency
IADC	Inter-Agency Space Debris Coordination Committee
LEO	Low Earth Orbit
PMD	Post Mission Disposal
STELA	Semi-analytic Tool for End of Life Analysis

1. Introduction

The number of launches, and hence the population of objects orbiting around the Earth is growing in recent years [1]. The increasing number of satellites has also led to the increase of breakup events (both explosions and collisions), which generated a large number of new fragments increasing the risk in specific region of the space environment. In addition, the general growth will likely accelerate with the introduction of large constellations in low Earth orbit (LEO), composed by low-cost, small satellites to provide broadband internet services to the world, posing a threat to the future sustainability of the space environment. Indeed, even though they will provide many benefits, like the access to internet to zones of the planet where there is lack of it, they will cluster a huge number of satellites in restricted region of the space. New or updated guidelines are needed to manage this new type of mission architecture (like the one presented by the Inter-Agency Space Debris Coordination Committee (IADC) [2]). Thanks to this and to efficient operations and management mitigation strategies the risk can be lowered [3].

Many past works analysed both the long- and short-term effect associated to the introduction of large constellation of the space population [3] [4] [5] [6], concluding that in order to lower the risk, a careful analysis on the Collision Avoidance Manoeuvre (CAM) capabilities and on the Post Mission Disposal (PMD) is required.

In this work, the THEMIS software tool, developed at Politecnico di Milano in collaboration with Deimos Space within an ESA-funded project, is used to assess the impact of a constellation [7]. As reference, the OneWeb constellation is considered in the analyses.

The paper is organised as following: Section 2 recalls the main features of the index evaluation adopted in THEMIS, Section 3 is devoted to the discussion on the distribution of the population of active objects, Section 4 introduces the main characteristic of the OneWeb constellation used in the test case presented in Section 5. A conclusive section summarises the main achievement and future works.

2. Environmental index

The evaluation of the index is performed using the THEMIS software tool, developed at Politecnico di Milano in collaboration with Deimos Space within an ESA-funded project. Here the main features are recalled. The space debris index is defined as a risk indicator, and follows the approach proposed in Letizia et al. [8]. The formulation is composed by a probability term (*p*), which quantifies the collision probability due to the space debris background population and the explosion probability of the analysed object, and a severity term (*e*) associated to the effects of the fragmentation of the analysed object on the population of active objects. The index is computed at a single time epoch as

$$\mathrm{I} = p_c \cdot e_c + p_e \cdot e_e \tag{1}$$

where p_c and p_e represent the collision and explosion probabilities, and e_c and e_e represent the collision and explosion effects, respectively. Depending on the operational status of the object, or on specific cases, the index can be computed twice at each epoch to account for the CAM capabilities of the satellite and its efficacy (ranging from 0 to 1).

A grid approach is used for the computation of the effect (both collision and explosion) and probability (just the collision) parameters. The grid is expressed in terms of Keplerian orbital elements, and for the LEO region the semi-major axis and the inclination are considered as study parameters [9] [10]. The explosion probability term is instead computed exploiting a survival estimator [11]. Moreover, historical and current data (e.g., physical properties) about the analysed objects are retrieved from the ESA DISCOS database [12].

2.1 Probability of collision

The probability of collision (p_c) is evaluated adopting a flux-based model of the space debris environment and exploiting the analogy with the kinetic gas theory [13] as follows

$$p_c(t) = 1 - e^{-N(t)} \tag{2}$$

where the number of impacts $N(t)$ can be estimated [14]

$$N(t) = \varphi \cdot A_c \cdot \Delta t \tag{3}$$

φ the average flux of space debris in 1/m^2/years, A_c the cross-sectional area of the object in m^2, and Δt the time span considered in year. ESA MASTER 8 is used to compute the flux and the averaged impact velocity on the grid defined before. The former is retrieved for different values of the debris size (in this work ranging from 1 mm to 10 m), while the latter is evaluated defining the target orbit using the bin edges of the grid, while randomly setting the other orbital parameters, and weighting each possible impact velocity according to the associated debris flux. As only catastrophic collisions are considered in the analyses, the impact velocity is used to determine a lower bound on the debris size and, consequently, on the magnitude of the flux used to compute the collision probability.

2.2 Probability of explosion

The probability of explosion (p_e) is evaluated analysing historical fragmentation available in DISCOS (considering accidental, propulsion, electrical, and unknown events, only) and by separating payload and rocket bodies. For each category, a series of bus types and rocket body families are considered (including two classes for generic payloads and rocket bodies which are not included in the other ones). The Kaplan-Meyer estimator [15] [16] is used to estimate the survival rate as

$$\hat{S}(t) = \prod_{i:t_i \le t} \left(1 - \frac{d_i}{n_i}\right) \tag{4}$$

where t_i is the time when at least one explosion happened, d_i the number of explosions at time t_i, and n_i the survived objects up to time t_i.

Then, the cumulative explosion probability is computed as

$$p_e(t) = 1 - \hat{S}(t) \tag{5}$$

2.3 Effect of fragmentation

The effect terms are evaluated starting from the analysis on the distribution of the operational satellites (i.e., the active objects within the population of objects

around the Earth), whose properties (e.g., orbital elements and physical properties) are acquired from DISCOS. The analysis is performed looking at the distribution of the cross-sectional area on a grid of 25 km in semi-major axis and 5° in inclination. The cumulative cross-section is computed for each cell of the grid and the bins containing up to 90% of the total cross-section are selected to host a target. The orbital parameters of the targets are equal to the centre of the bin, while the area and the mass are equal to the average value of the objects in the bin.

The second step is to generate a fragmentation (either a catastrophic collision or an explosion) for each cell in the same grid using the NASA standard breakup model [17], and by propagating the generated cloud of fragments through a continuum approach [18]. The cumulative collision probability between the generated fragments and the representative targets is computed over a time span of 15 as

$$e = \frac{1}{A_{TOT}} \sum_{i=1}^{N_t} P_c(t = 15ys) A_i \tag{6}$$

where A_{TOT} is the overall spacecraft's' cross-section, A_i is the cumulative cross-section of the objects belonging to the i-th bin, and P_c is the collision probability.

Depending on the type of breakup, three different maps will be generated: one for the collision (catastrophic), one for the explosion considering the breakup of a payload, and one for the explosion considering the breakup of a rocket body.

2.4 Debris index of a mission

To assess the impact of the entire mission, the value of the index is evaluated over the entire lifetime period as

$$I_t = \int_{t_o}^{t_{EOL}} I\,dt + \alpha \int_{t_{EOL}}^{t_e} I\,dt + (1 - \alpha) \int_{t_{EOL}}^{t_f} I\,dt \tag{7}$$

where t_o is the starting epoch, t_{EOL} is the epoch at which the operational phase ends, t_e is the epoch at which the disposal ends, t_f is the epoch at which the object would naturally decay from its initial orbit, I is the index value computed using Eq.(1), and α is a parameter associated to the reliability of the PMD strategy (ranging from 0 to 1). The first contribution of Eq.(7) refers to the operational phase of the object, the second to the PMD manoeuvre and the third to the natural decay from the operational state; the latter is considered if the PMD is not successful (i.e., $\alpha \neq 1$) or is not performed.

3. LEO active objects distribution and effects maps

For the purpose of this work, the maps described in Section 2.3 are generated considering three different populations:

- Population of objects where all the Starlink and OneWeb satellites are removed;
- Population of objects where all the Starlink satellites are removed, while OneWeb's are included;
- Population of objects considering all the objects.

The information on the operational satellites refers to data available on 30th June 2022 in DISCOS. The objective is to observe how the representative targets, and the associated effect maps, are influenced by the inclusion of large constellations.

Figure 1 shows the explosion effect map and the representative targets (in red) used to compute it when the constellations are not included in the set. From the figure it is possible to observe the presence of two areas (one around 800 km and one around 1400 km) where the effect terms is higher than 0. Moreover, in each region presents one peak (being the highest one in the sun-synchronous region at around 800 km). Figure 2 shows the updated maps when including the OneWeb constellation in the representative targets. As visible, the inclusion of OneWeb partially changes the representative targets (i.e., by removing some of them), including a new one in the bin containing the constellation (in black). This is due to the fact that a limit on the 90% of the total cross-sectional area is set, therefore if more objects are added, they may take that 90% up and some representative targets of the previous evaluation are then removed. These new targets generate a third vertical band in effect map at around 1200 km of altitude (which corresponds to the altitude of OneWeb). Looking at the value of the maximum peak, it is evident that the latter has decreased from the previous map. This behaviour is likely associated to the change in the total cross-sectional area when including the constellation (i.e., in this case an increase). Since the effect is rescaled according to the total cross-sectional area of the active objects, changing this value (and in parallel the number and position of the targets) would lead to a change in the value of the peak (as visible from Eq. (6)). The same is observed when including the Starlink constellation

(Figure 3) in the population used to generate the representative targets. The latter decrease in number due to the high cross-sectional area associated to Starlink, which overcomes the one of other bins. This change in the target affects also the shape of the effect map, shifting the peak at lower altitude and higher inclination. It is important to state that the peak is not exactly at the same altitude of Starlink because the fragments generated at this altitude will re-enter faster, thus lowering the impact on the population in time. However, also in this map the peak is lower than the previous case.

It is therefore necessary to think about a strategy to better deal with this change in the peak value. Possible solutions could be to change the method of the representative targets update (avoiding too many new inclusion or exclusions), or to change the rescaling method considering a relative area and no more the total cross-sectional area (thus avoiding problem in large changes of it, due to the inclusion of many new objects, or the removal of them).

In addition, looking at all the maps, it is possible to observe that the peak is symmetric with respect to the 90° inclination with respect to the location of the representative targets. This behaviour could suggest that adding new satellites in an already crowded region does not pose a threat to other satellites. However, a second peak (smaller than the other one) is always generated in the region of the target, and thus the inclusion of a huge number of objects would increase that peak.

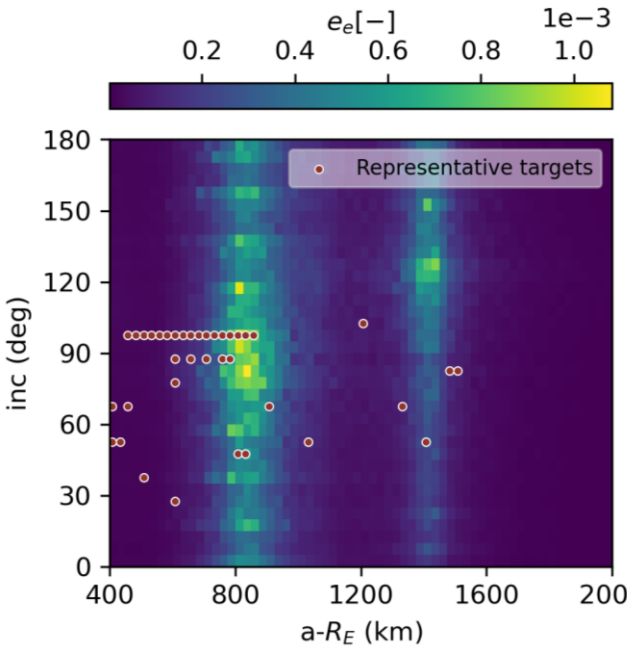

Figure 1. Explosion effect maps with representative targets (red dots) - no constellation.

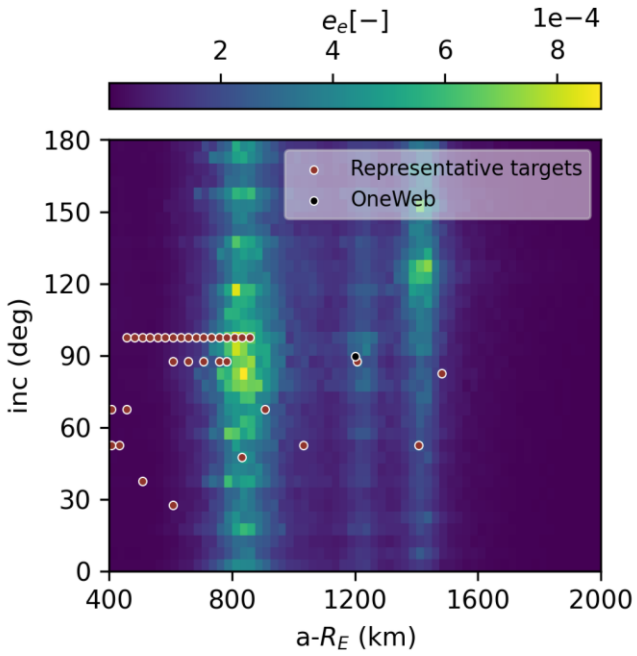

Figure 2. Explosion effect maps with representative targets (red dots) - OneWeb.

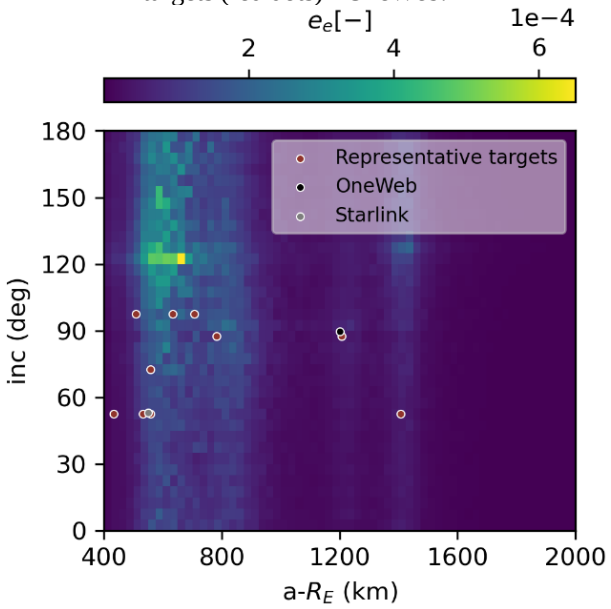

Figure 3. Explosion effect maps with representative targets (red dots) - OneWeb and Starlink.

Then, it is important to mention that, even though the effect map is a useful tool for the evaluation of the severity of the possible fragmentation on the space environment population, it probably lacks information. A way to improve them could be the inclusion of a feedback effect, which would take into account not only the effect of the fragmentation of the analysed objects, but also the effect of the fragmentation of the already in-orbit objects on it.

4. OneWeb-like constellation scenario definition

A OneWeb-like constellation is analysed as test case. The evaluation is performed considering the first generation of the constellation, which counts a total of 648 satellite subdivided in 18 orbital planes [3]. The main characteristics of the constellation are summarised in Table 1. Figure 4 shows the geometry of the OneWeb constellation (for the first phase of the mission) considering the characteristics described before.

Table 1. OneWeb constellation main features.

Name	Altitude [km]	Inclination [deg]	Orbital planes	Satellites
OneWeb	1200	87.9	18	648

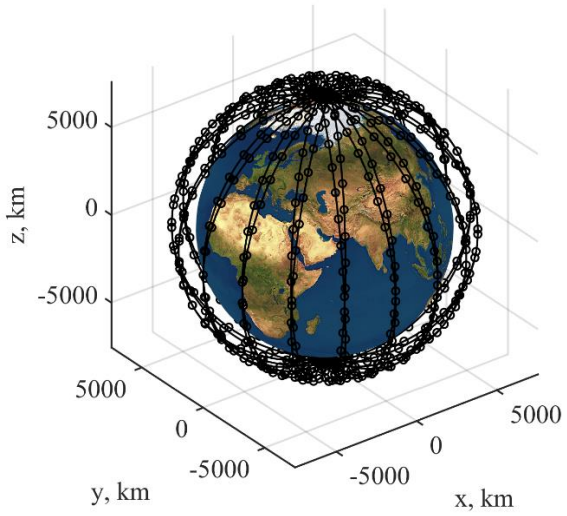

Figure 4. Geometry of the first generation of the OneWeb constellation.

For the assessment of the impact of the mission, three phases are defined for each satellite: orbit raising, operational, and End of Life (EOL). The orbit raising is analysed starting from the data available in SpaceTrack [19], which refers to one of the already launched satellites (NORAD ID 49083). The orbital parameters for this phase are extracted from the information available in the TLEs and used for all the considered satellites. The orbital parameters for the operational phase are considered as fixed and are set as 1200 km for the orbit altitude (considering a circular orbit) and 89.7° for the orbit inclination. The other parameters are not taken into account, as the index calculation only considers inclination and altitude. The PMD strategy consist in lowering the orbit altitude to 1100 km and then performing a disposal manoeuvre to set the perigee of the orbit to 245 km. The study of the PMD is performed using the Semi-analytic Tool for End of Life Analysis (STELA) [20]. For this study case, the constellation is considered to be operative for 50 years from the first launched satellite. The constellation is considered to be deployed starting on the 23nd January 2020.

The index of the constellation is compared with two other missions. The first one refers to the Envisat satellite, considering an orbit altitude of 780 km and an orbit inclination of 98.5°, which refers to the values at the beginning of the constellation deployment. The comparison is not performed considering the nominal mission of Envisat, while considering the operational status of this satellite at the time of the deployment of the constellation. In this way the comparison will be made over the same time period. The second mission is based on the study of a single satellite of the OneWeb constellation which, however, has an operational phase equal to the operative one of the constellations.

5. Index evaluation

This section presents the results on the computation of the index for the OneWeb-like constellation. As stated in Section 4, the index level of the constellation is compared with other mission, each of which is analysed considering two scenarios. In the first, the index is evaluated using the effect maps in which the OneWeb and Starlink constellations are not included, while in the second the index is evaluated using the effect maps including OneWeb (discarding again Starlink).

Figure 5 shows the evolution over time of the index of a single satellite of the OneWeb-like constellation considering an operational lifetime of 5 years. As can be seen from the image, adding the constellation in the background increase the level of the index during the operational phase. This may not be true for the orbit raising or the EOL phases due to the change in the distribution of the effect level in the maps.

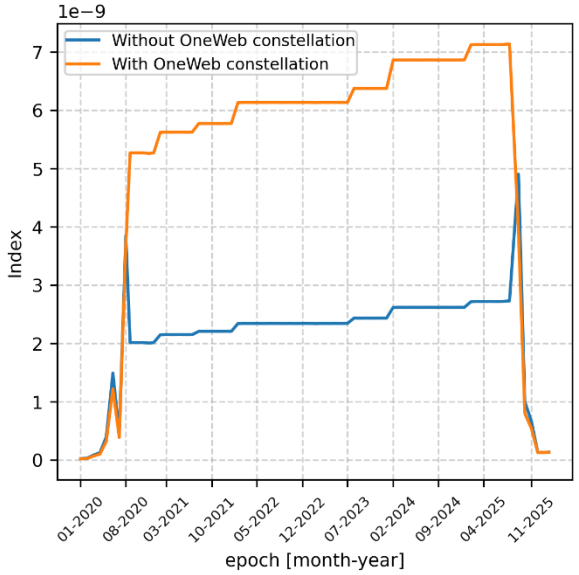

Figure 5. Index evolution over time for a single satellite of the OneWeb-like constellation.

Then, looking at the total index associated to the mission (thus also accounting for the reliability of the PMD phase), the results are summarised in Table 2. Total index of the analysed missions. The index evaluation of each mission (when considering a single satellite) is evaluated using Eq. (7), and assuming a PMD reliability of 0.9. For the evaluation of the index of the constellation an additional step is performed, that is the count of the number of satellites that will take part in the mission. At the end of the deployment phase, 648 satellites will orbit in the region of the constellation. The index of this in is preformed using the maps that does not include the constellation. Then, assuming a replenishment every 5 years (which is the nominal lifetime), another 5832 satellites must be considered. This time, the index is computed considering the effect maps that includes OneWeb.

Looking at the results in Table 2, it is possible to observe that the index of Envisat decreases with the introduction of the constellation. This is due, as discussed in Section 3, to the change in the effect maps when including OneWeb. Indeed, the introduction of constellation increased the level of the total cross-sectional area, thus reducing the value of the effect in the region around the Envisat (about 780 km). Then, analysing the value of the impact associated to a single satellite of the OneWeb-like constellation, the index of a single satellite (both the 5 years and the 50 years) increases when the constellation is considered in the population of active objects. In this case, as already stated (see Figure 1 and Figure 2), the introduction of OneWeb created a new column in the effects map (and consequently a new relative peak) around the region of its deployment, where the value of the effect is higher than before. Finally, the total index associated to the entire constellation mission resulted to be two orders of magnitude higher than the Envisat (which is the highest value among the single-satellite mission analysed). This result shows how the impact of new constellation (especially the larger one) will represent a much more difficult challenge, highly influencing the space environment around the Earth.

Table 2. Total index of the analysed missions.

Satellite	Index
Envisat (no constellation)	6.90E-04
Envisat (constellation)	5.56E-04
OneWeb single satellite (5 year – no constellation)	7.87E-07
OneWeb single satellite (5 year - constellation)	2.04E-06
OneWeb single satellite (50 year – no constellation)	3.31E-06
OneWeb single satellite (50 year - constellation)	8.68E-06
OneWeb constellation	1.24E-02

A way to reduce the value of the index would be to consider a more stringent requirement on the PMD reliability. Indeed, as visible in Figure 6, the total index decreases (as expected) when a higher value for the PMD reliability is considered.

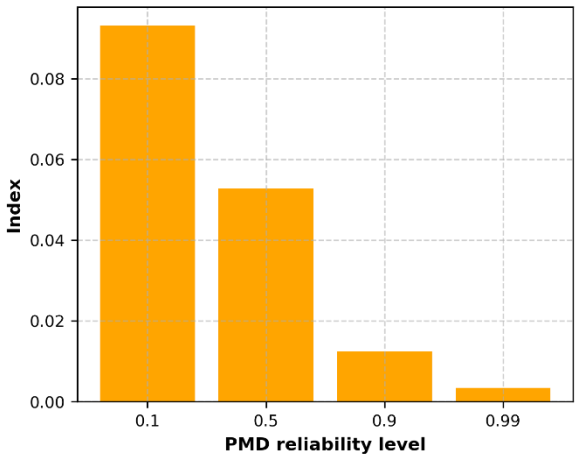

Figure 6. Comparison between different PMD reliability values for the index computation of the constellation.

However, it is also important to note that in the previous analysis, the failure of a single satellite is only accounted in the PMD reliability. Differently, when a failure occurs, a new satellite must be launched to

replace the other one thus increasing the total number of satellites in orbit, and consequently the level of the index.

6. Conclusions

The deployment of large constellation composed by small satellites is going to change the population of the objects orbiting around the Earth.

The aim of this work was to analyse the impact that these constellations will have on the space environment, focusing on the LEO region. As also stated in past works, constellations will bring benefits, but their design must be done properly and looking at the long-term sustainability of the space. Results showed that the introduction of the constellations is going to generate area at risk both in the region of the constellation itself but also in other region (mainly in terms of orbit inclination), thus influencing the selection of the location of future mission. This is already visible if the index evaluation is carried out considering or absence of the constellations, which in the latter case show lower values for the missions analysed.

Future work will perform more in-depth analysis, trying to compare constellations characterised by different architectures and location in the space.

Acknowledgements

This research has received funding from the European Space Agency contract 4000133981/21/D/KS and the European Research Council (ERC) under the European Union's Horizon 2020 research and innovation programme (grant agreement No 679086 – COMPASS).

References

[1] ESA Space Debris Office, "ESA's Annual Space Environment Report," 2022. [Online]. Available: https://www.sdo.esoc.esa.int/environment_report/Space_Environment_Report_latest.pdf.

[2] "IADC, 2021a. IADC Space Debris Mitigation Guidelines," [Online]. Available: https://www.iadc-home.org/documentspublic/filedown/id/5249.

[3] A. Rossi, A. Petit and D. McKnight, "Short-term space safety analysis of LEO constellations and clusters," *Acta Astronautica,* no. 175, p. 476–483, 2020.

[4] B. Bastida Virgili, J. C. .Dolado, H. G. Lewis, J. Radtke, H. Krag, B. Revelin, C. Cazaux, C. Colombo, R. Crowther and M. Metz, "Risk tospacesustainabilityfromlargeconstellations ofsatellites," *ActaAstronautica,* no. 126, p. 154–162, 2016.

[5] L. Olivieri and A. Francesconi, "Large constellations assessment and optimization in LEO space debris environment," *Advances in Space Research,* no. 65, p. 351–363, 2020.

[6] C. Pardini and L. Anselmo, "Environmental sustainability of large satellite constellations in low earth orbit," *Acta Astronautica,* no. 170, p. 27–36, 2020.

[7] C. Colombo, M. Trisolini, A. G. L. Muciaccia, J. L. Gonzalo, S. Frey, B. Del Campo, F. Letizia and S. Lemmens, "Evaluation of the Space capacity share used by a mission," in *73nd International Astronautical Congress (IAC)*, Paris, France, 2022.

[8] F. Letizia, S. Lemmens, B. Bastida Virgili and H. Krag, "Application of a debris index for global evaluation of mitigation strategies," *Acta Astronautica,* no. 161, p. 348–362, 2019.

[9] C. Colombo, M. Trisolini, J. L. Gonzalo, L. Giudici, S. Frey, K. Emma, N. Sánchez-Ortiz, F. Letizia and S. Lemmens, "DESIGN OF A SOFTWARE TO ASSESS THE IMPACT OF A SPACE MISSION ON THE SPACE ENVIRONMENT," in *ESA, 8th European Conference on Space Debris*, Virtual, 2021.

[10] C. Colombo, M. Trisolini, J. L. Gonzalo, L. Giudici, S. Frey, K. Emma, N. Sánchez-Ortiz, B. Del Campo, F. Letizia and S. Lemmens, "Assessing the impact of a space mission on the sustainability of the space environment," in *72nd International Astronautical Congress (IAC)*, Dubai, United Arab Emirates, 2021.

[11] E. L. Kaplan and P. Meier, "Nonparametric Estimation from Incomplete Observations.," *Acta Astronautica,* vol. 53, no. 282, pp. 457-481., 1958.

[12] "ESA DISCOS database," [Online]. Available: https://discosweb.esoc.esa.int/.

[13] D. S. McKnight, "A Phased Approach to Collision Hazard Analysis," *Advances in Space Research,* vol. 10, pp. 385-388, 1990.

[14] D. Kessler, "Derivation of the collision probability between orbiting objects: the

lifetimes of Jupiter's outer moons," *Icarus*, vol. 48, no. 1, pp. 39-48, 1981.

[15] M. Jankovic and F. Kirchner, "Taxonomy of LEO space debris population for ADR capture methods selection," in *Stardust Final Conference*, Springer International Publishing, 2018, pp. 129--144.

[16] E. c. a. a. e. m. d. driver, "Letizia, F.; Lemmens, S.; Krag, H.," *Acta Astronautica*, vol. 173, pp. 320-332, 2020.

[17] NASA, "Proper implementation of the 1998 NASA breakup model," *Orbital Debris Quarterly News*, vol. 15(4), p. 4–5, 2011.

[18] L. Giudici, M. Trisolini and C. Colombo, "Phase space description of the debris' cloud dynamics through continuum approach," in *73rd International Astronautical Congress*, Paris, France, 2022.

[19] "SpaceTrack," [Online]. Available: https://www.space-track.org/documentation. [Accessed 23 August 2022].

[20] V. Morand, J. C. Dolado-perez, H. Fraysse, F. Delefie, J. Daquin and C. Dental, "Semi-Analytical Computation of Partial Derivatives and Transition Matrix Using STELA Software," in *6th European Conference on Space Debris*, Darmstadt, Germany, 2013.